JBC Papers in Press. Published on April 24, 2001 as Manuscript C100162200

Functionally different agonists induce distinct conformations in the G protein coupling domain of the β_2 adrenergic receptor

Pejman Ghanouni[1,2], Zygmunt Gryczynski[4], Jacqueline J. Steenhuis[1], Tae Weon Lee[1], David L. Farrens[5], Joseph R. Lakowicz[4], and Brian K. Kobilka[1,2,3]

[1]Howard Hughes Medical Institute, [2]Department of Molecular and Cellular Physiology and [3]Division of Cardiovascular Medicine, Stanford University Medical School, Stanford, California 94305. [4]Center for Fluorescence Spectroscopy, Department of Biochemistry and Molecular Biology, School of Medicine, University of Maryland, Baltimore, Maryland 21201. [5]Departments of Biochemistry and Molecular Biology, Oregon Health Sciences University, Portland, Oregon 97201.

Address correspondence to:

Brian Kobilka

Phone: 650 723 7069

Fax: 650 498 5092

E-mail: kobilka@cmgm.stanford.edu

Running title: Agonist-specific conformations of the β_2 adrenoceptor

Summary

G protein coupled receptors (GPCR) represent the largest class of drug discovery targets. Drugs that activate GPCRs are classified as either agonists or partial agonists. To study the mechanism whereby these different classes of activating ligands modulate receptor function, we directly monitored ligand-induced conformational changes in the G protein-coupling domain of the β_2 adrenergic receptor (β_2AR). Fluorescence lifetime analysis of a reporter fluorophore covalently attached to this domain revealed that, in the absence of ligands, this domain oscillates around a single detectable conformation. Binding to an antagonist does not change this conformation, but does reduce the domain's flexibility. However, when the β_2AR is bound to a full agonist, the G protein coupling domain exists in two distinct conformations. Moreover, the conformations induced by a full agonist can be distinguished from those induced by partial agonists. These results provide new insight into the structural consequence of antagonist binding and the basis of agonism and partial agonism.

Introduction

G protein coupled receptors (GPCRs) are nature's most versatile biological sensors and are responsible for the majority of cellular responses to hormones and neurotransmitters, as well as for the senses of sight, smell and taste. Our current models of the mechanism of GPCR activation by diffusible agonists have been deduced from indirect measures of receptor conformation, such as G protein or second messenger activation (1-4). These indirect assays of GPCR activity provide only limited insight into the agonist-induced structural changes that define the active state of the receptor.

To elucidate of the mechanism of GPCR activation by diffusible agonists, we developed a means for directly monitoring the active conformation of purified, detergent-solubilized β_2 adrenergic receptor (β_2AR) by site-specific labeling of an endogenous cysteine (Cys265) with fluorescein maleimide (FM-β_2AR) (5). Based on homology with rhodopsin (6), Cys265 is located in the third intracellular loop (IC3) at the cytoplasmic end of the transmembrane 6 (TM6) α helix (Fig. 1A). Mutagenesis studies have shown this region of IC3 to be important for G protein coupling (7,8). An environmentally sensitive fluorophore covalently bound to Cys265 is therefore well positioned to detect agonist-induced conformational changes relevant to G protein activation. The effect of agonists and partial agonists on the fluorescence intensity of FM-

β_2AR correlates well with their biological properties (5). Binding of the full agonist isoproterenol induces a conformational change that decreases the fluorescence intensity of FM bound to Cys265 by ~15% (Fig. 1B), while binding of partial agonists results in smaller changes in intensity and binding of an antagonist has no effect (5).

Agonist-induced movement of FM bound to Cys265 was characterized by examining the interaction between the fluorescein at Cys265 and fluorescence quenching reagents localized to different molecular environments of the receptor. The results of these experiments are most consistent with either a clockwise rotation of TM6 and/or a tilting of the cytoplasmic end of TM6 toward TM5 (5). Our findings suggest that the conformational changes associated with β_2AR activation are similar to those in rhodopsin (9) and indicate a shared mechanism of GPCR activation.

These results provide insight into the nature of the structural changes that occur upon agonist binding. However several mechanistic questions remain. Using conventional spectroscopy, we observe no change in the fluorescence intensity from FM−β_2AR upon antagonist binding. This could indicate that antagonists do not alter receptor structure or that the structural changes are not detectable by FM bound to Cys265. Of greater interest is the structural basis of partial agonism. Partial agonists induce a smaller change in intensity of FM-β_2AR than do full agonists.

Two models could explain this observation. If we assume that the receptor exists in two functional conformational states, inactive or active, then a partial agonist may simply induce a smaller fraction of receptors to undergo the transition to the active state than does the full agonist. Alternatively, partial agonists may induce a conformation distinct from that induced by full agonists. Conventional fluorescence spectroscopy, which represents an average intensity over a population of fluorescent molecules, does not allow us to distinguish between these two models. We therefore used fluorescence lifetime spectroscopy, which is capable of distinguishing substates within a population of fluorescent molecules, to look for ligand-specific conformational states. Our results indicate that partial agonists and agonists induce distinct conformations. Moreover, we observe structural effects of antagonist binding that could not be detected by conventional spectroscopy. These results help elucidate the structural mechanisms which underlie ligand efficacy.

Experimental Procedures

Fluorescence spectroscopic studies of the β_2*AR*—Construction, expression and purification of human β_2AR were performed as described (10). Purified, detergent-solublized wild-type receptor was labeled with fluorescein maleimide (FM; Molecular Probes) as previously described (5). The labeling procedure resulted in incorporation of 0.6 mol of FM per mol of receptor. Fluorescence spectroscopy experiments were performed on a SPEX Fluoromax spectrofluorometer with photon counting mode using an excitation and emission bandpass of 4.2 nm. Approximately 25 pmol of FM-labeled β_2 adrenergic receptor was diluted into 500 μl of 200 mM Tris, pH 7.5, 500 mM NaCl, 0.1% NDM, 100 mM mercaptoethanolamine (MEA). Excitation was at 490 nm and emission was measured from 500 to 599 nm with an integration time of 0.3 s/nm for emission scan experiments. For time course experiments, excitation was at 490 nm and emission was monitored at 517 nm. For anisotropy studies, fluorescence intensities were measured with excitation and emission polarizers in horizontal (H) and vertical (V) combinations. The G factor was calculated from the ratio of the intensities (I) of I_{HV}/I_{HH} and the anisotropy (r) was calculated from $r = (\frac{I_{VV} - GI_{VH}}{I_{VV} + 2GI_{VH}})$. For studies measuring ligand effects, no difference was observed when using polarizers in magic angle conditions. Unless otherwise indicated, all experiments were performed at 25 °C and the sample always underwent constant stirring. The volume of the added ligands was ≤ 1% of total volume, and fluorescence intensity was corrected for this dilution in all experiments shown. All of the compounds tested had an absorbance of less than 0.01 at 490 and 517 nm in the concentrations used, excluding any inner filter effect in the fluorescence experiments.

Fluorescence lifetime analysis of fluorescein labeled β_2*AR*—To determine fluorescence lifetimes, approximately 250 pmol FM-β_2AR was diluted in 1.5 ml of 200 mM Tris, pH 7.5, 500 mM NaCl, 0.1% NDM, 100 mM MEA and incubated for 10 min at 25 °C with or without ligand. Fluorescence lifetimes were measured using a frequency-domain 10 GHz fluorometer equipped with Hamamatsu 6-μm microchannel plate detector (MCP-PMT) as previously described (11). The instrument covered a wide frequency range (4 - 5000 MHz), which allowed detection of lifetimes ranging from several nanoseconds to a few picoseconds. Samples were placed in a 10-mm path-length cuvette. The excitation was provided by the frequency-doubled output of a cavity-dumped pyridine-2 dye laser tuned at 370 nm synchronously pumped by a mode-locked argon ion laser. Sample emission was filtered through Corning 3-72 and 4-96 filters. For the reference signal, DCS in methanol (463 ps fluorescence lifetime) was observed through the same filter combination. The governing equations for the time-resolved intensity decay data were assumed to be a sum of discrete exponentials as in $I(t) = I_o \sum_i \alpha_i e^{t/\tau_i}$, where $I(t)$ is the intensity decay, α_i is the amplitude (pre-exponential factor) and τ_i is the fluorescence lifetime of the *i*-th discrete component; or a sum of Gaussian distribution functions as in the equation $I(t) = I_o \sum_i \alpha_i \tau e^{t/\tau}$ and $\alpha_i(\tau) = \frac{1}{\sigma\sqrt{2\pi}} e^{-\frac{1}{2}(\frac{t-\tau}{\sigma})^2}$ where τ is the center value of the lifetime distribution and σ is the standard deviation of the Gaussian, which is related to the full width at half-maximum by 2.354 σ. In the frequency domain, the measured quantities at each frequency ω, are the phase shift (φ_ω) and demodulation factor (m_ω) of the emitted light versus the reference light. Fractional intensity, amplitude, and lifetime parameters were recovered by a non-linear least squares procedure using the software developed at the Center for Fluorescence Spectroscopy. The measured data were compared with calculated values ($\phi_{c\omega}, m_{c\omega}$) and the goodness of fit was characterized by $\chi_R^2 = \frac{1}{\upsilon} \sum_\omega (\frac{\phi_\omega - \phi_{c\omega}}{\delta\phi})^2 + \frac{1}{\upsilon} \sum_\omega (\frac{m_\omega - m_{c\omega}}{\delta m})^2$, where υ is the number of degrees of freedom and $\delta\phi$ and δm are the uncertainties in the measured phase and modulation values, respectively. The sum extends over all frequencies (ω).

Results and Discussion

Using fluorescence lifetime spectroscopy to study ligand-induced conformational changes in the β_2AR.

The β_2AR was purified and labeled at Cys265 with fluorescein maleimide to generate FM-β_2AR as previously described (5). We examined ligand-dependent changes in fluorescence lifetime of FM-β_2AR in an effort to identify the existence of agonist-specific conformational states. Fluorescence lifetime analysis can detect discrete conformational states in a population of molecules, while fluorescence intensity measurements reflect the weighted average of one or more discrete states. Based on the changes in steady-state fluorescence intensity we observed, we predicted that ligand-induced conformational changes in the receptor would alter the fluorescence lifetime of the fluorophore. Fluorescence lifetime, τ, refers to the average time that a fluorophore which has absorbed a photon remains in the excited state before returning to the ground state. The lifetime of fluorescein (nanoseconds) is much faster than the predicted off-rate of the agonists we examined (μs - ms), and much shorter than the half-life of conformational states of bacteriorhodopsin (μs) (12), rhodopsin (ms) (13,14) or of ion channels (μs - ms) (15). Therefore, lifetime analysis of fluorescein bound to Cys265 is well-suited to capture even short-lived, agonist-induced conformational states.

Antagonist binding narrows the distribution of fluorescence lifetimes

Data from fluorescence lifetime experiments on FM-β_2AR bound to different drugs at equilibrium were analyzed in two ways. Traditionally, fluorescence decays are fit to single and multiple discrete exponential functions and the best fit determined by χ^2 analysis (Table 1). This discrete component analysis assumes that the receptor exists in one or a few rigid protein conformations and does not accurately reflect the dynamic nature of proteins. Proteins that are functionally in a single conformational state actually undergo small conformational fluctuations around a minimum energy state (16) and these small structural perturbations can lead to small changes in the environment around an attached fluorophore. These perturbations are thought to reflect local unfolding reactions within the three dimensional structure of proteins (17). Such flexibility in protein structure can be modeled using fluorescence lifetime distributions (18), wherein the width of the distributions reflects the conformational flexibility of the protein (Fig. 2). The mobility of fluorescein relative to the receptor is minimal, as determined by its high measured anisotropy (r = 0.30 ± 0.02, n = 3), and therefore would be expected to contribute little to the width of the lifetime distribution. Thus, the width of the distribution can be attributed to conformational flexibility in the receptor itself.

Lifetime analysis of unliganded FM-β_2AR reveals a single, flexible state. This is indicated by both the single, broad Gaussian distribution of lifetimes centered around 4.2 ns (Fig. 2, black trace), and the discrete component analysis, where the fluorescence decay rate of FM-β_2AR in the absence of any drug is best fit by a single exponential function (Table 1). Binding of the neutral antagonist ALP to FM-β_2AR does not significantly change the fluorescent lifetime (Table 1), but does narrow the distribution of lifetimes (Fig. 2, red trace), suggesting that ALP stabilizes the receptor and reduces conformational fluctuations. This interpretation is consistent with the results of experiments demonstrating that the β_2AR is more resistant to protease digestion when bound to ALP (19).

Agonists and partial agonists induce distinct conformations

Unexpectedly, binding of the full agonist ISO promotes conformational heterogeneity. In the presence of saturating concentrations of ISO, FM-β_2AR has two distinguishable fluorescence lifetimes (Fig 2, green trace, and Table 1) representing at least two distinct conformational states. The long lifetime component is only slightly longer than the lifetime observed in the absence of drugs; however, the distribution is narrower than that observed in the presence of the antagonist ALP (Fig.2, compare green and red traces). In contrast, the distribution of the short lifetime component observed in the presence of ISO is relatively broad, suggesting that there is considerable flexibility around Cys265 in this agonist-induced conformation.

We next examined the effect of the partial agonists salbutamol (SAL) and dobutamine (DOB) on the fluorescence lifetime of FM-β_2AR. Similar to ISO, we observed two lifetimes when the receptor was bound to saturating concentrations of SAL and DOB (Table 1, Fig. 3). The long lifetime component found in the presence of these two partial agonists is indistinguishable from that observed in the ISO-bound receptor; however, the short lifetime component found in both the SAL- and DOB-bound receptor is statistically different from that for the ISO-bound receptor. We observe a strong correlation between a reduction in fluorescence intensity of FM bound to Cys265 and drug efficacy (5), and shortening of the average fluorescence lifetime is associated with a reduction in fluorescence intensity. Therefore, the short lifetime, found only in the presence of agonists, likely represents the G protein activating conformation of FM-β_2AR.

The different short lifetimes for the full agonist (ISO) and the partial agonists (SAL and DOB) indicate different molecular environments around the fluorophore and therefore represent different, agonist-specific active states. The narrowing and rightward shift of the long lifetime component following binding of both agonists and partial agonists indicate that this lifetime also reflects an agonist-bound state, but most likely represents a more abundant intermediate state that would not be expected to alter greatly the intensity of FM bound to Cys265. It is possible that the number of conformations that we observe in these experiments represent only a few of the possible conformations that can be stabilized by drugs. Moreover, while the overlapping short lifetime distributions of SAL and DOB (Fig.3B and Table 1) suggest that they induce similar conformations, it is possible that a conformationally sensitive probe positioned elsewhere on the receptor could distinguish between DOB- and SAL-bound receptors states.

Models of GPCR activation

According to the prevailing two-state model of GPCR activation, receptors exist in an equilibrium between a resting (R) state and an active (R*) state which stimulates the G protein (20-22). Agonists preferentially enrich the R* state, while inverse agonists select for the R state of the receptor. Neutral antagonists possess an equal affinity for both states and function simply as competitors. In this simple system, functional differences between drugs can be explained by their relative affinity for the single active R* state (Fig. 4A). Alternatively, differences in efficacy between drugs can be due to ligand-specific receptor states (23-25). Based on our lifetime experiments, we propose a model with multiple, agonist-specific receptor states, wherein activation occurs through a sequence of conformational changes. Upon agonist binding, the receptor undergoes a conformational change to an intermediate state (R') that is associated with a narrowing and rightward shift in the long lifetime distribution. The less abundant active state, represented by the short lifetime, is different for the full agonist ISO (R*) and the partial agonists DOB and SAL (R^x). The relatively slow, temperature-dependent rate of change of fluorescence intensity following agonist binding and the rapid rate of reversal by antagonist ((5) and Fig. 1B) suggest that transitions from the intermediate state to the active state are relatively rare high energy events. It is likely that *in vivo* the active conformation is further stabilized by interactions between the receptor and its cognate G protein G_s. Thus, one might expect the proportion of receptor in the active state to be greater when the receptor is coupled with G_s.

Conclusions.

Our results have implications for drug discovery and efforts to obtain high resolution crystal structures of GPCRs. The conformational flexibility observed in the ligand-free receptor (Fig. 2) may make it particularly challenging to obtain crystals in the absence of a bound ligand. Of greater concern, the existence of two conformational states in the presence of saturating concentrations of full and partial agonists (Fig. 3) will impact efforts to obtain a high-resolution structure of the active, agonist-bound receptor. If such an agonist-bound structure is obtained, it will likely represent the more energetically stable of the two conformations and may not be the maximally active conformation. Thus, the use of such a structure for rational drug design efforts may have significant limitations. In support of this contention, recent structural analyses of the intermediate conformational states of the proton pump bacteriorhodopsin have revealed discrepancies attributed to energetic inhibition of conformational states within the three dimensional crystal (12,26). Finally, our results indicate that GPCRs are relatively plastic. The number of conformations that we observed in these experiments may represent only a few of a larger spectrum of possible conformations that could be stabilized by drugs. Thus, it may be possible to identify even more potent agonists or agonists that can alter G protein coupling specificity.

Acknowledgements: Brian Kobilka would like to thank Robert Lefkowitz, Henry Bourne, Lee Limbird, and Jurgen Wess for helpful comments on the manuscript. Pejman Ghanouni would like to acknowledge Gayathri Swaminath and Zhiping Yao for their assistance with protein purification.

References

1. Tota, M. R., and Schimerlik, M. I. (1990) *Mol Pharmacol* **37**(6)**,** 996-1004
2. Selley, D. E., Sim, L. J., Xiao, R., Liu, Q., and Childers, S. R. (1997) *Mol Pharmacol* **51**(1)**,** 87-96
3. Krumins, A. M., and Barber, R. (1997) *Mol Pharmacol* **52**(1)**,** 144-54
4. Perez, D. M., Hwa, J., Gaivin, R., Mathur, M., Brown, F., and Graham, R. M. (1996) *Mol Pharmacol* **49**(1)**,** 112-22
5. Ghanouni, P., Steenhuis, J. J., Farrens, D. L., and Kobilka, B. K. (2001) *Proc Natl Acad Sci U S A* (In Press)
6. Palczewski, K., Kumasaka, T., Hori, T., Behnke, C. A., Motoshima, H., Fox, B. A., Le Trong, I., Teller, D. C., Okada, T., Stenkamp, R. E., Yamamoto, M., and Miyano, M. (2000) *Science* **289**(5480)**,** 739-45
7. O' Dowd, B. F., Hnatowich, M., Regan, J. W., Leader, W. M., Caron, M. G., and Lefkowitz, R. J. (1988) *J Biol Chem* **263**(31)**,** 15985-92
8. Liggett, S. B., Caron, M. G., Lefkowitz, R. J., and Hnatowich, M. (1991) *J Biol Chem* **266**(8)**,** 4816-21
9. Farrens, D. L., Altenbach, C., Yang, K., Hubbell, W. L., and Khorana, H. G. (1996) *Science* **274**(5288)**,** 768-70
10. Gether, U., Lin, S., and Kobilka, B. K. (1995) *J Biol Chem* **270**(47)**,** 28268-75
11. Laczko, I. G. G., Gryczynski, Z., Wiczk, W., Malak, H., and Lakowicz, J. R. (1990) *Rev. Sci. Instrum.* **61,** 2331-2337
12. Subramaniam, S., and Henderson, R. (2000) *Nature* **406**(6796)**,** 653-7
13. Farahbakhsh, Z. T., Hideg, K., and Hubbell, W. L. (1993) *Science* **262**(5138)**,** 1416-9
14. Arnis, S., Fahmy, K., Hofmann, K. P., and Sakmar, T. P. (1994) *J Biol Chem* **269**(39)**,** 23879-81

15. Hoshi, T., Zagotta, W. N., and Aldrich, R. W. (1994) *J Gen Physiol* **103**(2)**,** 249-78

16. Frauenfelder, H., Sligar, S. G., and Wolynes, P. G. (1991) *Science* **254**(5038)**,** 1598-603

17. Freire, E. (2000) *Proc Natl Acad Sci U S A* **97**(22)**,** 11680-2 [MEDLINE record in process]

18. Gratton, E., Alcala, R., and F.G. Prendergast. (1989) in *Fluorescent Biomolecules: Methodologies and Applications* (Jameson, D. M., ed), pp. 17-32, Plenum Press, New York

19. Kobilka, B. K. (1990) *J Biol Chem* **265**(13)**,** 7610-8

20. Samama, P., Cotecchia, S., Costa, T., and Lefkowitz, R. J. (1993) *J Biol Chem* **268**(7)**,** 4625-36

21. Lefkowitz, R. J., Cotecchia, S., Samama, P., and Costa, T. (1993) *Trends Pharmacol Sci* **14**(8)**,** 303-7

22. Leff, P. (1995) *Trends Pharmacol Sci* **16**(3)**,** 89-97

23. Kenakin, T. (1997) *Trends Pharmacol Sci* **18**(11)**,** 416-7

24. Tucek, S. (1997) *Trends Pharmacol Sci* **18**(11)**,** 414-6

25. Strange, P. G. (1999) *Biochem Pharmacol* **58**(7)**,** 1081-8

26. Sass, H. J., Buldt, G., Gessenich, R., Hehn, D., Neff, D., Schlesinger, R., Berendzen, J., and Ormos, P. (2000) *Nature* **406**(6796)**,** 649-53

Figure Legends

Figure 1. *a.* Schematic diagram of the secondary structure of β_2AR illustrating the fluorescein maleimide (FM) labeling site at Cys265.

b. Effect of the full agonist (-)-isoproterenol (ISO) on fluorescence intensity of FM-β_2AR. Purified, detergent-solubilized β_2AR was labeled with FM at Cys265 and examined by fluorescence spectroscopy. Change in intensity of FM-β_2AR in response to the addition of ISO followed by the reversal by the neutral antagonist (-)-alprenolol (ALP).

Figure 2. Effect of drugs on fluorescence lifetime distributions of FM-β_2AR. Fluorescence lifetimes were determined by phase modulation and lifetime distributions of FM-β_2AR were calculated in the absence of ligand (*black trace*), with the neutral antagonist ALP (*red trace*), or in the presence of the full agonist ISO (*green trace*). The mean lifetime and the full width at half maximum for the distributions are: No Ligand: τ = 4.21 ± 0.01 nsec, FWHM = 1.1 ± 0.1, χ^2 = 2.8; ALP: τ = 4.21 ± 0.01 nsec, FWHM = 0.7 ± 0.2, χ^2 = 2.9; ISO: τ_{LONG} = 4.36 ± 0.08 nsec, $FWHM_{LONG}$ = 0.5 ± 1.1, τ_{SHORT} = 0.76 ± 0.33 nsec, $FWHM_{SHORT}$ = 1.7 ± 1.2, χ^2 = 3.2.

Figure 3. Comparison of the effects of full and partial agonists on the fluorescence lifetime distributions of FM-β_2AR. *a*, The effect of the full

agonist ISO and partial agonists SAL and DOB on the lifetime distributions of FM-β_2AR are compared. *b.*, Expanded view of the short lifetime distributions shown in *a.* The mean lifetime and the full width at half maximum for the new distributions are: SAL: τ_{LONG} = 4.37 ± 0.04 nsec, $FWHM_{LONG}$ = 0.7 ± 0.3, τ_{SHORT} = 1.93 ± 0.24 nsec, $FWHM_{SHORT}$ = 0.7 ± 0.3, χ^2 = 2.1; DOB: τ_{LONG} = 4.38 ± 0.01 nsec, $FWHM_{LONG}$ = 0.4 ± 0.4, τ_{SHORT} = 1.78 ± 0.01, $FWHM_{SHORT}$ = 0.9 ± 0.6, χ^2 = 2.0.

Figure 4. Diagram of the two-state model of GPCR activation (20). *a,* **R** is the inactive conformation and **R*** is the active conformation capable of activating the G protein. The equilibrium between **R** and **R*** is influenced differently by agonists (ISO) and partial agonists (DOB). The width of the arrows reflects the rate constant. *b,* Diagram of a multistate model of GPCR activation. The agonist ISO and the partial agonist DOB both induce an intermediate state **R'**, as well as distinct G protein activating conformations **R*** and **R**^{x}, respectively. The neutral antagonist ALP induces a conformation **R°** that is functionally equivalent to **R** at activating the G protein G_s, but can be distinguished from **R** by susceptibility to digestion by proteases.

Table 1. Fluorescent lifetime data for FM-β_2AR in the presence and absence of drugs fit to discrete exponential functions. The observed fluorescence decay was resolved into one or more exponential components, with each component, $\boldsymbol{i}$, being described by τ_i and α_i, where α_i represents the fractional contribution of τ_i to the overall decay. The best fit to single or multiple components was determined by χ^2 analysis. If different agonists induce a single active state, then the fluorescence lifetime associated with that state (τ_{R*}) should be the same for different drugs and only the fractional contributions (α_{DRUG}) should differ. However, if there are agonist-specific conformational states we should observe unique, agonist-specific lifetimes (e.g. τ_{ISO}, τ_{SAL}, and τ_{DOB}).

	τ_1 (nsec)	τ_2 (nsec)	α_2	χ^2
NO DRUG	4.22 ± 0.02	-	-	2.9 ± 0.4
ALP	4.21 ± 0.01	-	-	3.1 ± 0.8
ISO	4.30 ± 0.01	0.77 ± 0.05	0.19 ± 0.03	3.3 ± 1.0
SAL	4.35 ± 0.02	1.45 ± 0.16	0.08 ± 0.01	2.0 ± 0.2
DOB	4.36 ± 0.01	1.68 ± 0.3	0.07 ± 0.01	1.8 ± 0.4

Figure 1

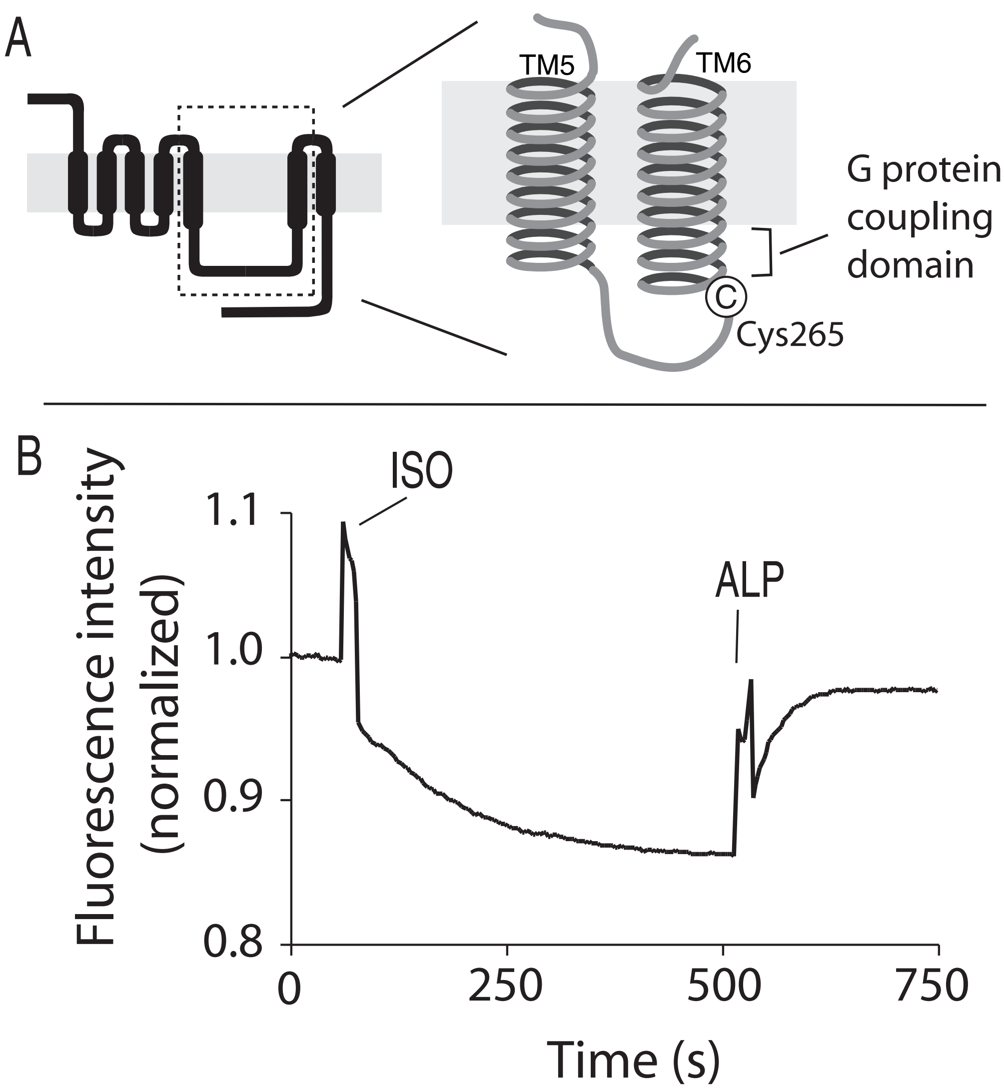
A
TM5
TM6
G protein
coupling
domain
C
Cys265
B
ISO
ALP
1.1
1.0
0.9
0.8
Fluorescence intensity
(normalized)
0
250
500
750
Time (s)

Figure 2

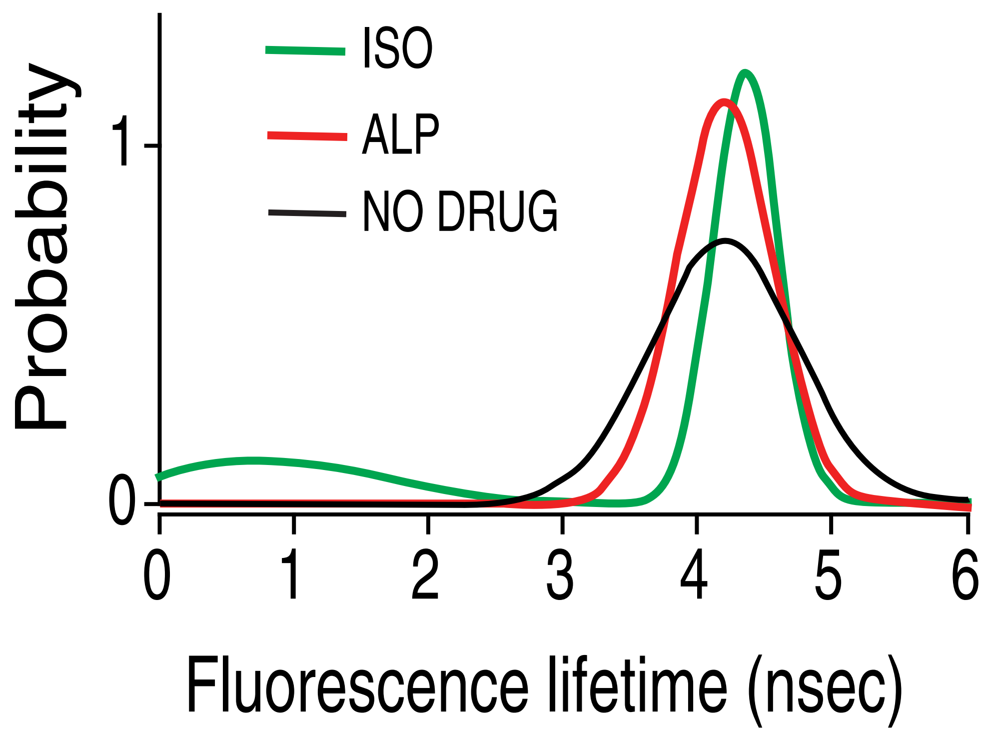

ISO
ALP
NO DRUG
Probability
1
0
0
1
2
3
4
5
6
Fluorescence lifetime (nsec)

Figure 3

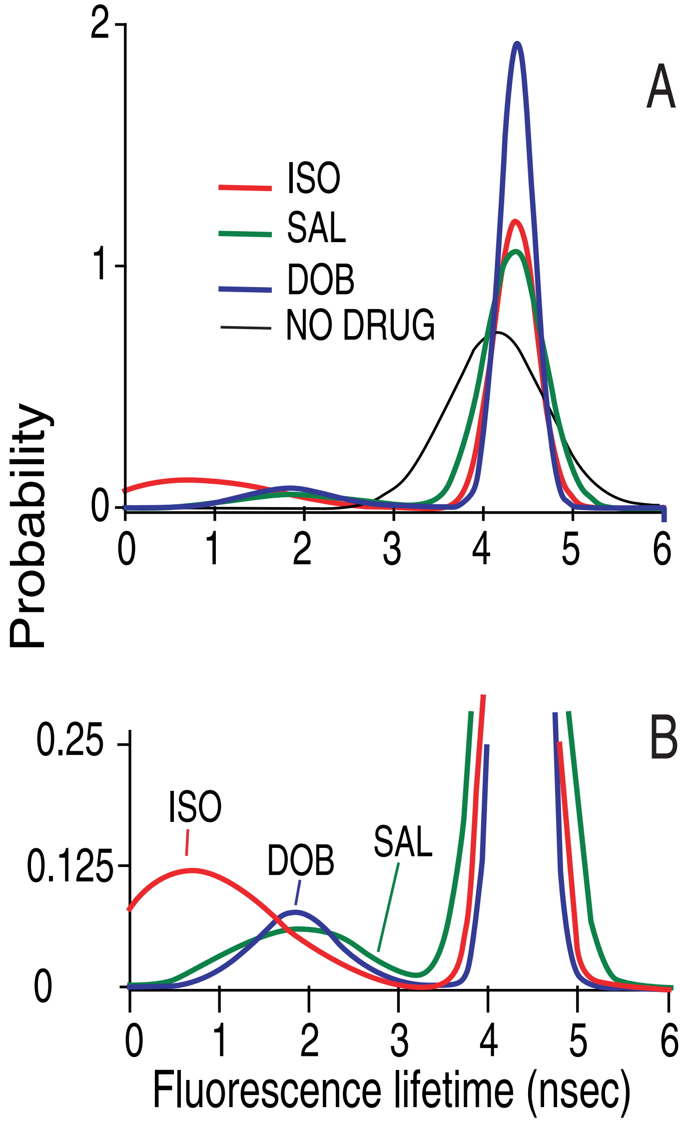
A
ISO
SAL
DOB
NO DRUG
Probability
2
1
0
0 1 2 3 4 5 6
B
0.25
0.125
0
ISO
DOB
SAL
0 1 2 3 4 5 6
Fluorescence lifetime (nsec)

Figure 4

A

$$R \rightleftharpoons R^*$$

$$RA_{LP} \rightleftharpoons R^*A_{LP}$$

$$RI_{SO} \rightleftharpoons R^*I_{SO}$$

$$RD_{OB} \rightleftharpoons R^*D_{OB}$$

B

$$R + A_{LP} \rightleftharpoons R^{o}A_{LP}$$

$$R + I_{SO} \rightleftharpoons R'I_{SO} \rightleftharpoons R^*I_{SO}$$

$$R + D_{OB} \rightleftharpoons R'D_{OB} \rightleftharpoons R^{x}D_{OB}$$